Optical Detector and Radiometer Standards

Optical Detector and Radiometer Standards

By

George P. Eppeldauer

Cambridge
Scholars
Publishing

Optical Detector and Radiometer Standards

By George P. Eppeldauer

This book first published 2021

Cambridge Scholars Publishing

Lady Stephenson Library, Newcastle upon Tyne, NE6 2PA, UK

British Library Cataloguing in Publication Data
A catalogue record for this book is available from the British Library

Copyright © 2021 by George P. Eppeldauer

All rights for this book reserved. No part of this book may be reproduced, stored in a retrieval system, or transmitted, in any form or by any means, electronic, mechanical, photocopying, recording or otherwise, without the prior permission of the copyright owner.

ISBN (10): 1-5275-6165-8
ISBN (13): 978-1-5275-6165-6

TABLE OF CONTENTS

Preface viii

1. Introduction 1

2. Absolute detectors 3
   2.1. Electrical substitution radiometers
      2.1.1. Room temperature ESRs
      2.1.2. Cryogenic ESCRs
   2.2. Si photodiode self-calibration
      2.2.1. Measurement of internal losses
      2.2.2. Measurement of external losses
      2.2.3. Hamamatsu-1337 single-element photodiodes
      2.2.4. 100 % quantum efficient Si trap detectors (QED)
      2.2.5. Comparison of single 1337 to UDT QED at 488 nm
      2.2.6. Temperature dependent UDT UV-100 self- calibration
      2.2.7. Elimination of response changes of UDT UV-100 diodes
      2.2.8. Spatial response uniformity and linearity of self - calibrated photodiodes
      2.2.9. Comparison of 1337-traps to ESCRs
      2.2.10. Internal quantum efficiency model for Si 1337
      2.2.11. Predictable quantum efficiency Si detector (PQED)
   2.3. Intrinsic detector standards
      2.3.1. Intrinsic absolute trap detectors
      2.3.2. Intrinsic relative response standards

3. Transfer standard detectors 41
   3.1. Si light-trap transfer standards
      3.1.1. Reflectance type Si trap
      3.1.2. Si tunnel trap
         3.1.2.1. Opto-mechanical design
         3.1.2.2. Electronic characteristics
         3.1.2.3. Loop gain characteristics
         3.1.2.4. DC mode measurements
         3.1.2.5. AC noise measurements

3.1.2.6. Comparison of DC and AC noise
3.1.2.7. Measurement accuracy issues
3.2. Transfer standard radiometers for UV to IR
3.2.1. Pyroelectric transfer standards
3.2.2. Radiometers for irradiance and radiance responsivity calibrations
3.2.2.1. Near-infrared transfer standards
3.2.2.1.1. Sphere-InGaAs radiometer characteristics
3.2.2.1.2. Use for calibrations
3.2.2.2. Short-wave infrared transfer standard
3.2.2.2.1. Design and application issues
3.2.2.2.2. EIGA transfer-standard characteristics
3.2.2.2.3. Detector signals from ambient objects
3.2.2.2.4. Use of traditional glass refractive optics
3.2.2.2.5. Use for calibrations
3.2.2.3. Ultraviolet transfer standard
3.2.2.4. Filter radiometer transfer standards

4. IR-enhanced Si transfer- and working-standards 124
4.1. IR-enhanced Si photodiode
4.2. Radiometric characteristics
4.3. Stability
4.4. Electrical characteristics
4.5. Expected responsivity uncertainty
4.6. Irradiance measurement mode
4.7. Application considerations

5. Typical working standard radiometers 138
5.1. UV meters
5.1.1. UV-A meters
5.1.2. UV-B and UV-C meters
5.2. Radiant- and luminous-flux meters
5.2.1. Visible to IR
5.2.2. Stability of Si detectors
5.2.3. Intrinsic standard of relative spectral response
5.3. Irradiance and illuminance meters
5.3.1. VIS to SWIR
5.3.1.1. Versatile mechanical and optical design
5.3.1.2. Stability of illuminance meters
5.3.1.3. Cooling and heating of detectors and filters
5.3.1.4. Spectral coverage, atmospheric transmission

5.3.1.5. Ext-InGaAs noise-equivalent irradiance
5.3.1.6. Electronic considerations
5.3.1.7. Extended-InGaAs stability
5.3.2. InSb for MW-IR
5.3.2.1. Optical mechanical design
5.3.2.2. Electronic design
5.3.2.3. InSb flashing and stability
5.3.2.4. Response versus frequency
5.3.2.5. Response nonlinearity
5.3.2.6. Signal range and noise floor
5.3.2.7. Spatial and angular response
5.3.2.8. Wide-range spectral responsivity measurement of InSb
5.3.3. MCT detectors for MW-IR
5.3.3.1. PV-MCT working standard
5.3.3.1.1. Large-area multi-junction PV-MCT detector
5.3.3.1.1.1. Spatial uniformity of response
5.3.3.1.1.2. Shunt resistance issues
5.3.3.1.1.3. Output signal and noise
5.3.3.1.1.4. Spectral responsivity
5.3.3.1.1.5. NEP improvement issues
5.3.3.2. PC-MCT working standard
5.4. Radiance and luminance meters
5.4.1. SWIR detectors in radiation thermometers
5.4.2. Other applications of SWIR radiance meters
5.5. Tristimulus photo/colorimeters
5.5.1. Design considerations
5.5.2. Design of filter combinations
5.5.3. Channel characteristics
5.6. Operational tests of radiometers

6. References 223

PREFACE

Improved detector technology in the past two decades opened a new era in the field of optical radiation measurements. An increased number of calibration and measurement facilities and procedures could be developed with lower measurement uncertainties using the newly developed detector/radiometer standards instead of traditionally applied source standards (blackbodies and lamps). Shrinking of the traditional source-based calibrations and the large increase of optical detector-based calibrations motivated the writing of this book series.

The book series is a comprehensive description of optical detector based radiometric practices. Instead of giving the traditional lexical-type tutorial information, a research-based material is systematically organized and described. The large number of examples cover modern detector applications in the field of radiometry, photometry, colorimetry, and radiation temperature measurements. All the discussed devices and applications have been implemented, realized, tested, verified, and evaluated. These applications are described to obtain uniform results with low measurement uncertainties. They are described with enough details to successfully repeat them by the readers/users. The applications and evaluations follow the recommendations of international standardization. The described subjects are detailed and distributed in five volumes.

Properties of radiometric quality detectors, their use and selection for optical radiometers, design considerations of radiometers and detector-based standards, description of spectral and broadband detector-based calibrations and measurements using modern setups based on the new radiometer standards are described for practicing scientists, engineers, and technicians.

The book series includes many hundreds of designs, drawings, measurement schemes, a large number of detector-based measurement and calibration setups, measurement equations and results, calibration-transfer and measurement methods/procedures all tested in practical applications.

In addition to reference level detector/radiometer calibrations, measurement of radiometric quantities used in practice (secondary laboratory and field applications), are discussed. Such quantities are radiant power, irradiance, and radiance. Measurement of spectral and broadband (integrated) quantities are discussed from 200 nm in the ultraviolet to 30 μm in the infrared.

All discussed calibrations and measurements are traceable to the System International (SI) units through National Measurement Institutes (NMI) and/or the discussed intrinsic detector standards.

Linear and traceable measurement of detector output signals, including DC and AC photocurrent (sub-scale) and voltage measurements, detector-amplifier gain-calibrations, and gain-linearity tests are discussed in detail.

Uncertainty determination/calculation methods of detector-based measurements are described. It is a general rule for the discussed large number of design and application examples, to keep the calibration/measurement uncertainties low.

The author thanks all the colleagues listed in the references at the end of each volume for their help and contribution to perform the discussed large number of measurements and evaluations.

Dr. George P Eppeldauer, author

1. INTRODUCTION

The standard devices for optical radiometric calibrations and measurements are either sources or detectors (optical radiometers). Two to three decades ago, all radiometric calibrations were performed against source standards. The primary source standards are blackbody sources of known temperature (fixed point blackbody). The International Temperature Scale of 1990 (ITS-90) [1] - before that, the International Practical Temperature Scale of 1968 (IPTS-68) - standardized the freezing-point temperature of molten metals utilized in black-body radiators. The spectral power distribution of a blackbody source at a given temperature can be calculated from Planck's Law. When radiometric devices (lamps or detectors) are calibrated against a black-body source, a long calibration (derivation) chain is used. The long chain is necessary because the optical radiation measuring geometry can change during the scale derivation and also the temperature has to be transformed from the low temperature of a fixed point blackbody to the high temperature of standard lamps. Also, the spectral power distribution of tungsten lamps is different than that of Planckian radiators. When the spectral power distribution of a test lamp is needed it is measured against a Planckian radiator using a monochromator and a variable temperature black-body source [2]. The results of the standard source-based scale derivations are radiometric standard lamps with known spectral power or irradiance distributions applicable for radiometric, photometric, pyrometric, and colour calibrations of sources, detectors, devices, and instruments. The uncertainty of the standard lamps (as a result of the long scale derivation) is in the order of one percent (wavelength dependent) with respect to the System International (SI) unit, the watt [3]. The stability of lamp standards is poor; therefore the uncertainty of a scale is increasing with the increasing number of the burning hours of the lamp standards. The reproducibility is also in the order of a percent and it is wavelength dependent too.

Synchrotron radiation sources (emitting under vacuum conditions) are also used as primary radiometric standards. The spectral radiant power of an electron storage ring can be calculated from the electron

energy, the magnetic induction, and the electron current stored in the ring. A synchrotron source covers a very wide wavelength range including IR, VIS, UV, VUV, and soft X-ray regions. The uncertainty for the calculation of the spectral radiant power through an aperture is about 0.2 % in the near IR and the visible range [4].

In the last three decades (from the 1980s), because of optical detector improvements, detector-based calibrations are increasing and source-based calibrations are shrinking. It was necessary to develop modern radiometers using the improved detectors for realizing, holding, and disseminating the new detector-based scales. In detector-based calibrations, the primary standard is an absolute (traceable to the watt) radiometer. The responsivity of an absolute radiometer for radiant power is known with uncertainties between 0.1 % and 0.01 % (k=2). The radiant power is a derived SI unit. Absolute radiometers (called also absolute detectors) are either electrical substitution radiometers or quantum efficient (self-calibrated) detectors. The absolute detectors, and the transfer and working standard radiometers used for radiometric calibrations and measurements are discussed in this volume.

The advantage of detector-based to source-based calibrations is a lower uncertainty in the scale realizations and the following scale distributions. The higher stability of the detectors (as compared to lamps) results in better long-term stability and reproducibility in radiometric, photometric, and colour measurements.

2. ABSOLUTE DETECTORS

Typically, radiometric calibrations are made against reference detectors. A reference detector is a detector standard with minimum measurement uncertainty of its spectral responsivity that is traceable to the SI unit(s). Traceability is usually obtained by purchasing standards calibrated by National Metrological Institutes (NMIs). The relative uncertainties associated with the spectral responsivity values of reference standards can be different depending on the type and performance of the device. They will also depend on the number of the scale derivation steps.

The detector standards with lowest measurement uncertainty are electrical substitution cryogenic radiometers (ESCR) [5]. Si trap detectors [6] and sphere-input InGaAs [7] or sphere-input extended InGaAs detectors are used as transfer standards. A radiant power value measured with an ESCR has an associated relative standard measurement uncertainty of close to 0.01 %.

The United Detector Technology (UDT) made model QED-200 Si trap detector includes three UDT UV-100 n-on-p inversion layer photodiodes[1]. The QED stands for quantum efficient detector. This trap detector can be used as transfer standard. The UV-100 photodiodes-based trap detectors can measure radiant power with a relative standard measurement uncertainty of 0.03 % between 440 nm and 460 nm without applying any bias voltage to the photodiodes [8]. Therefore, the QED-200 trap detectors are intrinsic (absolute or primary) standards between 440 nm and 460 nm. The response linearity of this trap detector is poor and it must be used below 100 μW. The linearity can be improved and the spectral range can be extended using a reverse bias voltage (self-calibration of these detectors is discussed below in Chapter 2.2.). Using the reverse bias to compensate for charge-pair recombination losses in the bulk region of silicon of these np-type Si photodiodes, the spectral range

[1] The mention of certain commercial products in this publication is for information purposes only and does not constitute an endorsement of the product by the author.

of the QED-200 can be extended [9]. The overall wavelength coverage of the QED-200 (as an absolute standard) is from 360 nm to 800 nm. The bias voltage requirement is 5 V at 600 nm and it increases to 90 V at 800 nm. The UDT reports +/- 0.1 % uncertainty (k=1) for the absolute responsivity in the above quantum-efficient wavelength range. However, a spatial non-uniformity of responsivity of about 0.1 % was measured by the author of this book at 500 nm within a circular aperture of 8 mm diameter. This uncertainty component should be included in the uncertainty budget of power responsivity measurements. The measured spatial non-uniformity is +/- 1 % relative to the center of the detector at 1000 nm. Another limiting factor for the QED-200 applications is the low (<10 MΩ) shunt resistance. High signal-gains (large feedback resistors in the current-to-voltage converter) produce high voltage-amplifications with the low shunt resistance for the input 1/f noise (introduced by the bias). The too high output noise can be a limiting factor for monochromator applications.

The UDT made QED-150 and several other trap detectors on the market are made from Hamamatsu 1337 p-on-n silicon photodiodes. These photodiodes are “quantum-flat” because they have external quantum efficiencies (EQE) that are constant to within 0.1 % from about 600 nm to 930 nm. The spectral responsivity of quantum detectors is proportional to their EQE and wavelength. The quantum flatness of these trap detectors could be extrapolated to 400 nm using the above mentioned silicon photodiode self-calibration technique [8] discussed in Chapter 2.2. These pn-type Si trap detectors are the preferred absolute detectors for the long-wave spectral region because they do not require a reverse bias to compensate for charge-pair recombination losses in the bulk region of the silicon. These pn-type Si trap detectors (using the 1337 photodiodes) can be used as intrinsic standards if a responsivity uncertainty of 0.15 % (k=2) is enough. Also, when improved uncertainties are needed, the spectral responsivity of the S1337 trap-detectors (with the constant relative spectral responsivity) can be calibrated against either a UDT QED-200 between 440 nm and 460 nm (as mentioned in Chapter 2.2.9) or an ESCR.

Usually, Si trap detectors are used as standards at NMIs and they are often optimized for an operation with intensity-stabilized laser sources. For example: Transfer standard Si trap detectors can be calibrated against ESCRs or reference trap detector standards. As

described below, the transfer standard trap detectors can utilize the physical model of the internal quantum efficiency for Hamamatsu 1337 silicon photodiodes [10] [11]. For radiant power responsivity, a relative standard measurement uncertainty of 0.03 % can be achieved on Si trap detectors between 405 nm and 920 nm using the model. These are the highest-level transfer standards for the silicon wavelength range that can be calibrated by NMIs.

Reflectance or transmission (tunnel) type trap detectors can be used as reference standards. These Si trap detectors are also discussed below. The advantage of tunnel-trap detectors is that the incident beam is entirely transmitted and there are no back reflections at the input. Stable optical components (such as glass filters) can be located at the front of the tunnel-trap detector that can be calibrated (e.g. for spectral transmittance) separately from the trap detector. Usually, trap detectors have a FOV of only a few-to-several degrees. If a source other than a laser beam is to be measured, the FOV of the trap-detector must be large enough not to vignette the incident beam (e.g. from a monochromator).

The trap arrangement improves the uniformity of the spatial responsivity compared to a single element photodiode, which is an important issue in radiant power mode measurements where the incident beam underfills the active area of the detector.

Sphere-input InGaAs transfer-standard detectors with a tilted input aperture (relative to the sphere axis) and a symmetrical photodiode arrangement (relative to the sphere axis and the incident beam spot) can have radiometric and electronic characteristics similar to silicon trap detectors. They can perform absolute responsivity calibrations with 0.05 % uncertainty in the 950 nm to 1650 nm wavelength range [7]. The design and performance of a sphere-input InGaAs detector is discussed in Chapter 3.2.2.1.1.

2.1. Electrical Substitution Radiometers (ESR)

Most of the national standard laboratories developed their ESRs. Gillham [12] showed first the major error sources in room temperature electrical substitution radiometry, such as non-uniformity of response across the radiation receiver, non-equivalence of the radiant and electrical heating, imperfect absorption and thermal conduction of black coatings, lead heating and polarity effects, heating of the radiometer housing and the imperfections of practical

diaphragms. National radiometric scales developed in the following years usually were based on new room temperature ESR designs in order to reduce the above error sources or to quantify them for correction purposes [5]. In the improved ESRs thermopiles were used as temperature transducers. Lithographic technics were also applied to produce the thermopile [13], and also in an electrically calibrated pyroelectric radiometer [14] pyroelectric material was applied instead of thermopile. The cavity versions of the ESRs have better spectral flatness of responsivity than the flat absorber types. Therefore, a range of room temperature, electronically balanced, cavity type electrical substitution radiometers (ESRs) were developed in the 1970s and 1980s. In ground based solar radiometry [15], a detector-based scale, The World Radiometric Reference (WRR), was established on absolute detectors in 1977 after the different ESR measurements agreed within 0.3% in terms of SI units. The first comparison between the WRR and SI scales showed an agreement of better than 0.03 % [16].

The block scheme of a thermal radiometer is shown in Fig. 1. The radiation absorbing receiver, A, made from a blackened cone or disk, has a thermal capacity of C. It converts the incident radiant power, P, into heat with a time constant, τ. The heat change is detected by a temperature sensor, S. The S (together with A) is connected to a heat sink, R, through a thermal conductance, G. The temperature of S and A without incident optical radiation is equal to the constant reference temperature, T_o, of R. The time (t) dependent temperature increase ΔT of S and A relative to T_o, for a sudden application of incident optical radiation, can be described:

$$\Delta T = \frac{P}{G}\left(1-e^{-t/\tau}\right) \qquad (1)$$

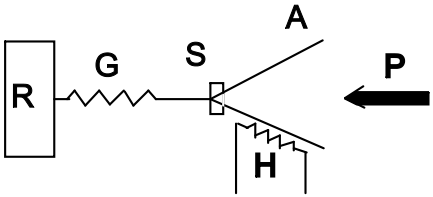

Fig. 1. Block scheme of a thermal radiometer.

where the time constant of the thermal radiometer is:

$$\tau = \frac{C}{G} \qquad (2)$$

After heat balance, $\Delta T = P/G$. Regular bolometers do not have heater, H. In ESRs the radiative heating is replaced with electrical heating using H. The current through the resistive coil of H is controlled until the same ΔT temperature increase is measured by S. Then the electrical heating power of receiver A is measured.

The minimum value of ΔT which can be measured, called minimum detectable temperature difference, is determined by the type and construction of the ESR. The range of P (especially the low end limit) can be adjusted by changing G. This adjustment should be done with care because change of τ can have an unwanted feedback for ΔT. E.g. decreasing G will increase ΔT and τ. However, increasing τ slows down the radiometer which may result in increased noise (1/f) in the radiometer measuring circuits. This way the minimum detectable temperature (because of higher noise) may increase.

2.1.1. Room temperature ESRs

In room temperature ESRs the heat sink, R, is not cooled, it is at ambient temperature. The receiver, A, can be either a target disk or a cavity. The target disk is a thermal diffuser, usually copper or silver, to which thermopiles, bolometer, or pyroelectric detector is attached on the back side. The front side has a radiation absorber, usually a black coating. The thermal diffuser can be heated by a heater which is insulated from the disk. The electrical heater can be a resistive element or an evaporated gold electrode [17]. These ESRs are used in null mode, with an electrical heating adjusted so that alternate electrical and radiant heating cycles produce the same temperature rise in the receiver as measured by the temperature sensor. The electrical heating power is measured by current and voltage leads attached to the heater. The incident radiant power can be determined from the measured electrical power after applying a number of small corrections. Lead heating typically accounts for 0.3 % of the total heating. The main correction to be applied is for radiation reflected from the black coating of the target disk. This may be several percent for black paints, or less than a percent for a gold-black surface. The

loss caused by the surface reflection can be reduced by applying a hemispherical mirror in front of the coated disk to return the reflected radiation to the receiver. This method is useful only when the coatings have high reflections. The non-equivalence of radiant and electrical heat power also limits the accuracy. The radiation produced heat must diffuse through the black paint and the disk to heat the thermopile. The thermal impedances for the radiant heat can cause greater losses to the surroundings for the radiant heating than for the electrical heating. For carbon black the radiant heating can be undervalued by about 0.4%. When gold black is used the loss is ten times smaller. This loss can be reduced to negligibly small by operating the gold-black coated detector in vacuum. In vacuum the thermal impedance to the surroundings increases.

In certain applications, two-cavity compensated ESRs [18] are used. The advantages of this ESR are its high absorptance and non-selectivity over a wide spectral region, thus increasing measurement accuracy. The conical cavity is made of copper, its length is 25 mm, the half vertex angle is 11.3^{o}, and the diameter of the opening is 10 mm. Coiled manganese heating wires are glued uniformly to the inner surface of the cavity, and the interior is then coated with 3M matt-black paint. In order to increase the sensitivity of the ESR, 102 pairs of thermocouples of nichrome-constantan, 0.1 mm diameter, are arranged uniformly in eight circles (12 for one) on the outer surface of the cavity. The responsivity of the ESR is 0.21 V/W and its time constant is about 15 s. In order to minimize fluctuations in the output voltage of the thermocouples, caused by the ambient temperature change, a compensating cavity is incorporated. The two conical cavities have the same thermal and electrical properties and are connected in series with opposing polarity. One of them is irradiated, the other serves only for thermal compensation and it is not irradiated. A precision entrance aperture of 7 mm diameter is located in front of the cavity. The heater winding is within this irradiated area in order to make the effect of the optical and electrical heating as equivalent as possible. The body of the ESR has a high heat capacity and a high heat conductivity so that, when irradiated by a radiating source, reradiation will be reduced to a minimum. At the same time the ESR itself is thermally shielded from its surroundings. The metal body is wrapped in a polytetrafluoroethylene sleeve to reduce the thermal effects caused by the ambient temperature changes. In order to make accurate radiant power measurements corrections were applied. The 0.11 to 0.14 %

measured cavity reflectance had to be corrected. Because of the thermal resistance of the 3M matt-black cavity coating a correction factor of 1.0007 was introduced. As the diameter of the aperture shield was larger than the diameter of the entrance aperture the irradiating light source overfilled the entrance aperture causing an additional temperature rise in the body. The correction factor for the excess heat of the heat sink, caused by the source irradiation, was 0.9994. The consistency of the absolute responsivities of a group of seven ESRs was evaluated and each ESR differed from the grand mean by 0.1% or less. The one year long-term irradiance measurement instability was better than 0.1%.

Thin film techniques were used in the ESRs fabricated at the National Research Council (NRC) of Canada. The first version incorporated a gold-black absorber, a chromium thin film heating element, a copper thermal diffuser, and a 28-junction chromium-nickel thin film thermopile on a glass-copper-ceramic substrate. The 0.07 V/W responsivity and the 100 nW NEP was improved in a second version [13]. Two, 6 um thick Mylar membranes were used. On the back of the front membrane a 13 um thick, 1 cm diameter copper disc was made by electroplating and photoetching; on the front of this membrane, from the membrane outward, a silver-bismuth thin film electrical heating element, a thin diluted Glyptal insulating layer, and a gold-black absorber was applied. On the back membrane a 30-junction silver-bismuth thermopile faced the front membrane and a high-reflector silver coating was evaporated on the other side of the back membrane. Response uniformity was improved here to 0.2% over a 0.7 cm^2 area by using symmetrical thermopile hot junction distribution. The heating element was confined to a circular region having the same diameter as the detector aperture (6 mm). Because of the high resistance bismuth heater (5000 ohm) the heat caused by the lead resistance (<1 ohm) was negligible. Gold-black was used as absorber because it has very low reflectance in the UV, visible, and near IR. As it also has a low thermal resistance, errors can be avoided due to nonequivalence effects between two forms of heating (radiant and electrical). The thermal diffuser between the two membranes also helps to eliminate nonequivalence errors between the two modes of heating. In the second version the main ESR characteristics, that is, responsivity, speed of response, and NEP, were improved about fivefold compared with the first version. These ESRs can achieve an overall accuracy of +/- 0.1% if correction is made for the nonabsorbed radiation.

Corrections are always necessary because of wavelength dependent reflectance changes of black coatings. Thermopiles and bolometers always need a black coat while pyroelectric detectors are often used in a form in which radiation absorption takes place in the pyroelectric crystal or ceramic chip rather than at its surface. However, this restricts the wavelength range in which the pyroelectric detectors are useful to that in which they are strongly absorbing. In order to extend the range and to provide an absorbing surface of known spectral absorptance it is necessary to apply a black coating. As an example, the reflectance of the popular gold-black may change between 0.2 % and 2 % in the 200 nm to 3000 nm spectral range. Blackened Ni-P has the lowest spectral reflectance, of about 0.16 %, which is relatively independent of wavelength between 400 and 1800 nm [19]. The black coating should be applied by a well-established technique which combines the highest possible absorptance over a wide wavelength range with low thermal capacity. In addition the thermal resistance of the black coating has to be low, so that all the power absorbed is transferred rapidly to the temperature sensing disk. Unfortunately, the preparation of black coatings appears to be very much a "black art" and reproducible coatings cannot be relied on even when they are prepared by the same person working in the same laboratory [20].

With properly designed room temperature ESRs radiant powers can be measured in a range of about 10 μW to a couple of mW with an uncertainty (k=1) of about 0.1%. The response time is limited by the thermal time constant of the receiver. The fastest ESR is the thin film type where the time constant can be as low as 3s. For disk and cavity type ESRs the time constant is several times larger.

2.1.2. Cryogenic ESCRs

In the past 2-3 decades electrical substitution cryogenic radiometers (ESCRs) were developed to operate at either liquid helium or liquid nitrogen temperatures. At very low temperatures, material properties are superb than at room temperature. The thermal diffusivity of the cavity at liquid helium temperature is three orders of magnitude greater than at room temperature [21]. This feature maintains isothermal conditions in the cavity, even if the cavity is large. At the same time the time constant of the cavity decreases [9]. Application of superconducting leads makes it possible to avoid corrections because of lead heating. The coupling between the receiver and its

surrounds becomes negligible. As a result of the improved features, there is no need for temperature balance corrections. Calibrations with these primary standard ESCRs are made at high radiant power levels therefore radiometric accuracy is more important than sensitivity. The ESCRs achieved responsivity uncertainties are in the order of 10^{-4}. This is an order of magnitude accuracy improvement relative to room temperature ESRs. ESRs and ESCRs have the advantage of near-constant absolute responsivity over a wide wavelength range, but they are generally slow to respond and are relatively insensitive.

In ESCRs the radiometric heating and electrical heating are also alternately applied to the thermal receiver of these radiometers. At a heat balance in the receiver the radiant power can be calculated from the measured electrical power. Using this substitution method, non-linearity, mid-term and long-term instabilities of cryogenic thermal sensors are canceled out. Non-equivalences in heat balance and uncertainties in electrical power measurements during short substitution time intervals determine the accuracy of radiant power measurements. Usually, the calibrations with these primary radiometric standards are made at high radiant power levels therefore radiometric sensitivity is a less important question.

ESCRs are also utilized in other application areas, such as in infrared (IR) applications and measurement of low-level optical radiations. In most of these applications they must have high sensitivities. There is a trade-off between accuracy and sensitivity [22]. Their spectrally flat (wavelength independent) responsivities are utilized in many applications such as spectrally total radiant power (thermal radiation) measurement of low temperature blackbody sources. In IR applications, especially spectral radiometric measurements, the power level at the output slit of a monochromator is low.

The construction of a cryogenic thermal radiometer is complex. In order to achieve the increasing expectations of different radiometric applications the construction of a cryogenic radiometer must be goal optimized. The thermal and electronic system designs are to be made in an interaction with each other. The goal is to find or develop cryogenic devices that can achieve the requested radiant power measuring criteria (accuracy, sensitivity, dynamic range, spatial uniformity, linearity, spectral flatness, etc) when they are used together with properly designed (matched) electronic measuring

circuits. The selection of the cooling temperature is another design consideration. In many applications liquid nitrogen temperatures can be more convenient than liquid helium temperatures.

If ΔT=1K for a full-scale measurement, and a dynamic range of a decade is needed, then ΔT=100 mK should be measured with an uncertainty of about 10^{-4}. This requires temperature instabilities in an ESCR of about 10 μK. The same instability level is required if the dynamic range of operation is three decades and the expected uncertainty is 1%. To measure these very small temperature changes cryogenic radiometers have to be used where the detectivity of the selected temperature sensor is very high.

The primary standard ESCR of NIST [23] is shown in Fig. 2. The liquid He cooled cavity can operate at 2 K. The liquid He container and the cavity are thermally shielded with an outside jacket (cold block) cooled to about 77 K using liquid Nitrogen. Power levels can be measured from μW to mW levels between 200 nm and 20 μm. A Si trap-detector transfer-standard can be moved into the beam-path with a translation stage to perform windowless power-scale transfer (for decreased uncertainties).

ESCRs are complicated and expensive. Usually, they are purchased and operated only when power responsivity uncertainties are required in the 0.01 % level. In order to perform 0.1 % (k=2) or higher uncertainties, less complicated reference detectors can be used.

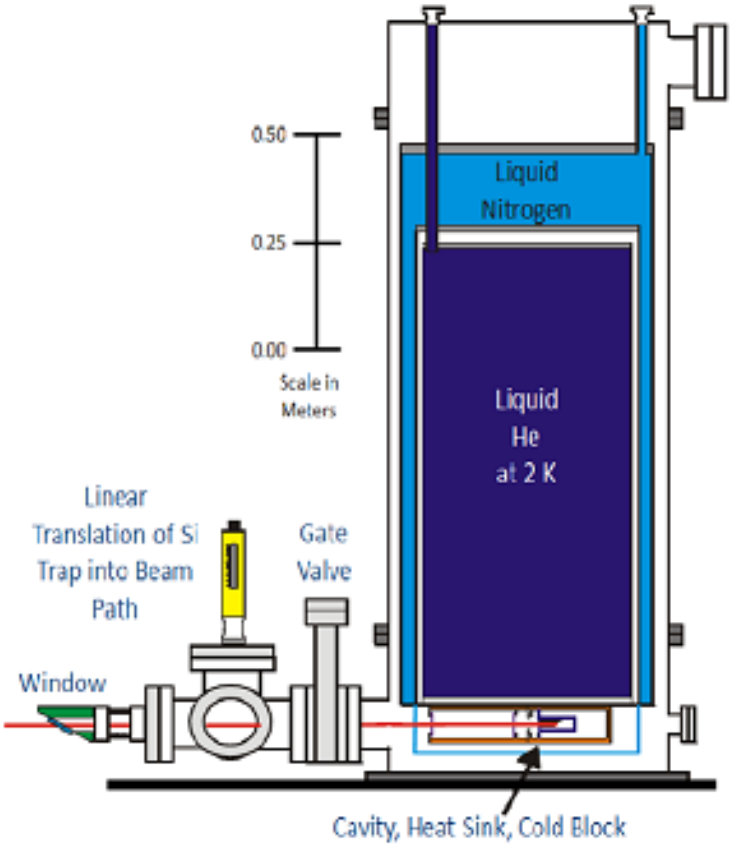

Fig. 2. Cross section of a cryogenic ESCR primary standard.

2.2. Si photodiode self-calibration

Self-calibration is a technique for determining the external quantum efficiency of a silicon photodiode from the material and device properties of the photodiode itself. A self-calibrated silicon photodiode is a radiometric absolute detector which does not require any additional calibration against other radiometric standards. The internal quantum efficiency of certain silicon photodiode models approximates the unity in part of the Si wavelength range. The absolute spectral response of those photodiodes could be determined

over that spectral region by a rather simple "self-calibration" technique. This technique involved measurements of the relative losses to deduce the departures of the internal quantum efficiency from unity. The self-calibration technique is relatively simple and the absolute accuracy of the self-calibrated silicon photodiodes can be in the order of 0.1%. This technique was introduced in the 1980s [24].

The absolute spectral response, s(λ), of a silicon photodiode at wavelength λ can be calculated from its external quantum efficiency, EQE(λ) using the relation

$$s(\lambda) = EQE(\lambda) \frac{e \lambda}{h c} \qquad (3)$$

where the elementary electron charge, e = 1.6021 * 10^{-19} Cb, the velocity of light, c = 2.997925 * 10^{8} m/s, the Planck's constant, h = 6.6256 * 10^{-34} W/s^2, and

$$EQE(\lambda) = [1-\rho(\lambda)]\varepsilon(\lambda) \qquad (4)$$

where ρ is the specular spectral reflectance of the silicon photodiode and ε is its internal quantum efficiency (IQE).

Both ρ and ε are to be determined from the device properties of a particular photodiode to be self-calibrated. For an ideal device ρ is zero and ε is unity. Both ρ(λ) and ε(λ) are to be determined from relative measurements that are called silicon photodiode self-calibration procedure.

The internal quantum efficiency, ε(λ), of a silicon photodiode can be less than unity because of recombination losses during normal operation of the photodiode. Recombination losses occur at two different locations in the photodiodes. In the front region the photo-generated carriers may recombine at the oxide-silicon interface instead of contributing to the photocurrent. The result is a decreased responsivity at short wavelengths. Similarly, recombination can happen in the bulk region of the silicon photodiode. This effect reduces the internal quantum efficiency from unity at longer wavelengths.

During the self-calibration procedure both the above mentioned internal (recombination) losses and the external (reflectance) losses are measured.

2.2.1. Measurement of internal losses.

Internal losses are due to recombination losses. Measurement of the recombination losses at the oxid-silicon interface is rather difficult. During these so-called oxide-bias measurements the relative response of the photodiode is measured under constant irradiation as a function of bias voltage applied to the oxide [25]. The ε_o internal quantum efficiency component is defined as the ratio of the photocurrent obtained with zero bias voltage across the oxide to that obtained with a bias voltage sufficient to saturate the photocurrent.

Originally, the apparent saturation of diode response with increasing oxide bias was taken as an indication that the recombination at the oxide-silicon interface had been completely eliminated. Later work showed that the saturation was associated with the flat band condition at the oxide-silicon interface rather than the elimination of interface recombinations [26]. A small fraction of the oxid-silicon interface recombination loss remained and was not completely eliminated.

As a result of numerical modelling of short-wavelength internal quantum efficiency of two types of p^+nn^+ silicon photodiodes, higher accuracies could be reached. Also, an uncertainty could be associated with the data reduction of the oxide bias measurement. In practical self-calibrations two different shallow junction p^+nn^+ (p on n) silicon photodiode types were applied. First, the older type, the EG&G UV444B photodiode, was self-calibrated using the oxid bias measurement. During an oxide bias measurement a negative bias voltage was connected to the SiO_2 front layer with a transparent water-drop electrode to repel the electrons which could be recombined by the positive charges trapped in the SiO_2 layer. First, the zero bias internal quantum deficiency (one minus the quantum efficiency) was calculated for a UV444B photodiode at 476.2 nm. The results obtained from the original assumption and a simulation were not accurate enough [27]. Using the same numerical photodiode modelling program [8] on a newer photodiode, the Hamamatsu 1337, the internal quantum deficiency could be accurately approximated over the 440 nm to 640 nm spectral range [27]. However, this

prediction has not been verified experimentally. If verified, this result should prove very useful in quantum efficiency interpolations involving the use of this type of photodiode and multiple reflectance (light trap) type detectors made from it. (The internal quantum efficiency of a 1337 photodiode is nearly unity in the long wavelength visible.) The front-region doping distribution of the Hamamatsu 1337 photodiode is different (shallower) in comparison with the UV444B photodiode. Though the uncertainties in the internal quantum deficiency associated with the diode-to-diode variations in doping profile are quite small for the 1337 type photodiode, the oxide-bias measurement was still less than ideal for self-calibration [28].

Both water electrodes and corona discharge have been used to apply oxide bias. Corona discharge was satisfactory only in very dry atmosphere [29]. Application of a water drop on the photodiode surface could permanently change both the reflectance [29], and the internal quantum efficiency. The internal quantum efficiency decreases in the blue wavelength range because of the changes (passivations) in the surface electron states [30, 31]. In order to avoid these changes the oxide bias measurement could be applied only once. After scale realization, the scale had to be maintained by a different photodiode calibrated against the self-calibrated one.

The oxide bias measurement could be avoided when an inversion layer (induced junction) type photodiode was selected for self-calibration. A frequently applied type was the UV-100 photodiode from United Detector Technology (UDT). The UDT UV-100 silicon photodiode is different from the UV444B and 1337 type photodiodes. It is an n on p photodiode. As a result of an ion implantation procedure positive charges are built into the SiO_2 front layer. Because of these positive charges the electrons are redistributed at the Si-SiO_2 interface. This is how an inversion layer is created relative to the p type substrate which is like a very shallow induced n^+p junction between the substrate and the oxide layer. The strong surface field repels the photo-generated minority carriers from the oxide-silicon interface before recombination occurs. Therefore the internal quantum efficiency is very close to unity at short wavelengths [32]. This is the basis for the use of the UDT Models QED 100 and QED 200 multiple reflection (light trap) radiometers [6], which contain modified UV 100 photodiodes as high accuracy absolute radiometric standards. According to the original assumption, the internal quantum efficiency of the UDT UV 100 photodiodes is unity in the

short wavelength visible. As the state of the art in absolute radiometry improved with time, this assumption became more questionable. When the internal quantum deficiency was simulated in this spectral range (between 400 and 500 nm) for a nominal UV-100 photodiode, made after 1986, a nominal internal quantum efficiency of 0.9997 +/- 0.0003 was received for the unbiased UDT UV-100 type photodiode in the 440 to 460 nm spectral region [28]. This result was considered a one-standard-deviation equivalent (k=1), rather than a limit of error, since the analysis was based on the results obtained for a single device. Outside the 440 nm to 460 nm spectral region, the uncertainties grew so rapidly that they were not really practical for high accuracy applications. The UDT UV 100 photodiode can be used as a high accuracy absolute detector in this limited spectral range without measuring the internal losses.

Reverse-bias measurements can be performed to measure the second type of photodiode recombination loss is the volume recombination in the weakly doped n layer between the p-n junction and the rear electrode under normal operation. The recombination here can be eliminated if the length of the depletion layer is extended towards the rear electrode by applying an external bias voltage serially connected to the photodiode. During a reverse-bias measurement, the relative response of the photodiode is measured under constant irradiation as a function of reverse bias voltage [25]. The ε_R internal quantum efficiency component is defined as the ratio of the photocurrent obtained with zero reverse bias voltage to that obtained with a reverse bias voltage sufficient to saturate the photocurrent.

Simulation of the reverse-bias measurement, based on the above modelling programs, does not work well enough with inversion layer (induced junction) photodiodes. No simulation programs were used for high accuracy applications [28].

2.2.2. Measurement of external losses

The largest external loss occurs because of the specular reflection of the photodiode front surface. Usually, the front surface of the photodiodes, used for self-calibration, is of optical quality. Therefore other external losses, such as the diffuse component of the reflectance, cause an error in the absolute spectral response measurement of << 0.1 % [24].

Measurement of the front surface reflectance of the photodiode is relatively simple if the applied beam is collimated. Usually, the self-calibration is made with a narrow, well collimated beam, and the photodiode active area is underfilled. This is a detector calibration in radiant power measurement mode. For radiometric applications the beam is usually monochromatic. Both laser and non-coherent sources can be used. When laser beams are used the intensity of the beam should be stabilized. If the monochromatic beam of a monochromator is used, the beam should be well collimated. Determination of the specular reflectance loss is easier if the beam is well collimated. Self-calibrations with uncollimated radiations can result in increased uncertainties [33, 34].

2.2.3. Hamamatsu-1337 single-element photodiodes

Self-calibrated single-element Hamamatsu 1337 silicon photodiodes can be used as standard (absolute) detectors if the uncertainty requirement from the standard detector is not better than 0.1 %. Self-calibrated 1337 photodiodes can be used as primary detector standards in the visible and in the near IR wavelength ranges.

As an example, the self-calibrations of three single-element Hamamatsu 1337 photodiodes are shown in Table 1. These self-calibrations were performed at 488 nm. The laser output power was 0.5 mW. To get high stability, a second silicon photodiode monitored the laser fluctuations and an analog divider was used to ratio the signal to the monitor signal.

Table 1

Self-calibration of three Model-1337 single-element Si photodiodes at 488 nm

	1337-1	1337-2	1337-3
ρ	0.3492	0.3453	0.3488
ε_R	1.000	1.000	1.000
ε_o	0.9980	0.9945	0.9960
EQE	0.6495	0.6511	0.6485

The EQE in Table 1 was calculated from Eq. 4. The reflectance, ρ, and the internal quantum efficiency components, ε_R and ε_o were measured (as discussed above). The bias voltages for both internal

quantum efficiency components were 40 V. ε_R=1.000 shows that the reverse bias voltage had no effect on the internal quantum efficiency at this short (488 nm) wavelength. However, the effect of the oxide bias for the internal quantum efficiency was significant. The standard deviation of the external quantum efficiency determination from repeated self-calibration measurements was 0.1 % for a given 1337 photodiode. The maximum difference among the three calculated external quantum efficiencies is 0.4 %.

The quantum efficiency of a 1337 photodiode between 700 and 920 nm is 0.1 % to 0.15 % less than unity [35] . The 1337 photodiodes are quantum flat in this long wavelength interval without any self-calibration. At short wavelength (488 nm), the 1337 photodiodes must be self-calibrated to achieve a high enough power measurement accuracy. This short wavelength accuracy achievement was checked against quantum efficient detectors. The purpose of this check was to see if the power measurement error at a short wavelength was comparable to the power measurement errors at long wavelengths where the errors are caused by the above mentioned 0.1 to 0.15 % photodiode quantum efficiency deviation.

2.2.4. 100 % quantum efficient Si trap detectors (QEDs)

In a trap detector three or more Si photodiodes are located inside of the detector, in a way to get multiple reflections for the incident beam. Most of the incident radiation is absorbed as a result of multiple reflections. This is how the reflectance loss of this detector is minimized. If the number of reflections within a trap detector is large enough the resultant reflection loss can be smaller than the other errors associated with the trap detector self-calibration.

The first trap detector design was made from four silicon inversion layer (UDT UV-100) photodiodes [6]. The windows of all four photodiodes were removed. Three photodiodes were set at 45^o to the incident beam so that the reflected beam from the first photodiode was incident on the second and so on. The fourth photodiode was perpendicular to the beam reflected from the third photodiode. This way the beam was reflected back along its original path. The input beam was incident on seven photodiode surfaces before exiting the trap detector. The area of each photodiode was 1 cm^2, circular. At the front (in the entrance plane) of the device, a 0.1 cm^2 aperture was located. The field of view at 1m from this aperture was an ellipse with

major and minor diameters of 5.0 and 2.7 cm, respectively. At 50 cm from the aperture the major and minor diameters were only 2.3 and 1.2 cm. The four photodiodes were connected parallel with each other and the sum of their currents was measured by a current to voltage converter. The applied inversion layer type photodiodes do not have recombination losses at the interface and in the front volume. The junction is induced by positive charges trapped in the SiO_2. The front region minority carriers (holes) are repelled from the SiO_2-Si interface by the trapped positive charge and swept across the junction by the field within the depletion region. This way the front region recombination loss is negligible. Short-wavelength photons will be entirely absorbed in the front region.

The only loss in a well-designed trap detector is due to recombination loss in the bulk region of the photodiodes. To eliminate this loss an external bias voltage must be connected serially to the parallel connected photodiodes.

The external quantum efficiency of an inversion layer silicon photodiode trap detector is unity in the short wavelength visible (with the uncertainty limits). Outside the 360 nm to 550 nm wavelength interval, the trap detector requires self-calibration. The self-calibration is simple because only the reverse-bias measurement is to be applied on the trap detector for the elimination of the recombination loss in the bulk region of the photodiodes. The longer the wavelength the higher bias voltage is necessary. At the longest wavelength, 800nm, where the reverse bias still works, the bias requirement is 90 V. The external quantum efficiency is about 1 % different from 100 % at this wavelength. Since the biased response of the trap detector is a straight line between 360 nm and 800 nm, it can be described mathematically. The absolute response for 100 % external quantum efficiency from Eq. 3 is

$$s = \lambda/1239.5 \qquad (5)$$

where s is expressed in A/W and the wavelength λ is in nm.

After the four-photodiode (inversion layer) trap detector (manufactured by UDT as Model QED-100) a three photodiode version was developed. This trap detector is called UDT QED-200. The minimum number of photodiodes for a polarization insensitive detector is three. Light not completely absorbed by photodiode 1 is reflected to photodiode 2 in a path encountering a total of five surfaces. The